

This document is confidential and is proprietary to the American Chemical Society and its authors. Do not copy or disclose without written permission. If you have received this item in error, notify the sender and delete all copies.

pH-Triggered Reversible Multiple Protein-Polymer Conjugation based on Molecular Recognition

Journal:	<i>The Journal of Physical Chemistry</i>
Manuscript ID:	jp-2015-066375.R1
Manuscript Type:	Article
Date Submitted by the Author:	07-Aug-2015
Complete List of Authors:	Liu, Juan; University of Basel, Department of Chemistry Postupalenko, Viktoriia; University of Basel, Department of Chemistry Duskey, Jason; University of Basel, Department of Chemistry Palivan, Cornelia; University of Basel, Chemistry Department Meier, Wolfgang; University of Basel, Department of Chemistry

SCHOLARONE™
Manuscripts

pH-Triggered Reversible Multiple Protein-Polymer
Conjugation based on Molecular Recognition

Juan Liu, Viktoriia Postupalenko, Jason T. Duskey, Cornelia G. Palivan, Wolfgang Meier**

Department of Chemistry, University of Basel, Klingelbergstrasse 80, Basel 4056, Switzerland

ABSTRACT: Polymer conjugation for protein based therapeutics has been developed extensively; but still suffers from conjugation leading to decrease in protein activity, and generates complexes with limited diversity due to general classical systems only incorporating one protein per each complex. Here we introduce a site specific non-covalent protein-polymer conjugation, which can reduce the heterogeneity of the conjugates without disrupting protein function, while allowing for the modulation of binding affinity and stability, affecting the pH dependent binding of the number of proteins per polymer. We compared classical one protein polymer conjugates with multiple protein polymer conjugates using His-tagged enhanced yellow fluorescence protein (His₆-eYFP) and metal-coordinated tris-nitrilotriacetic acid (trisNTA-Meⁿ⁺) in a site-specific way. trisNTA-Meⁿ⁺-His₆ acts as a reversible linker with pH triggered release of functional protein from the trisNTA functionalized copolymers. The nature of the selected Meⁿ⁺ and number of available trisNTA-Meⁿ⁺ on poly(N-isopropylacrylamide-*co*-tris-nitrilotriacetic acid acrylamide) (PNT) copolymers enable predictable modulation of the conjugates binding affinity (0.09-1.35 μ M), stability, cell toxicity, and pH responsiveness. This represents a promising platform that allows direct control over the properties of multiple protein polymer conjugates compared to the classical single protein polymer conjugates.

INTRODUCTION

Protein therapeutics is of high importance in almost every field of medicine.¹ However, there are still a number of challenges in the application of protein therapeutics that have to be overcome.^{1,2}

Therapeutic proteins exhibit low stability, fast renal clearance, enzymatic degradation, and are frequently immunogenic.³

An elegant way to overcome these problems is to conjugate polymers to proteins, which has been reported to improve protein stability, half-life, solubility, and reduce immunogenicity.⁴⁻⁸

However, such conjugation can lead to the alteration of the protein structure, resulting in a decrease or even complete inhibition of protein activity.^{9,10} An effective approach to overcome a loss of protein function is to design stimuli-responsive linkage between polymers and proteins.¹¹

This enables the linkage to be independent of the protein function, and therefore, cleavage of the protein from the polymer conjugate by a specific stimulus releases the intact and functional protein.¹¹⁻¹³ Currently, covalent attachment of polymers to proteins through stimuli-cleavable

linkers has mainly been developed.^{11,13-15} Non-covalent interactions with a stimuli-responsive nature are rarely applied for protein-polymer conjugation due to their instability.^{16,17} The interaction between metal-coordinated nitrilotriacetic acid (NTA-Meⁿ⁺) and His-tagged proteins is a promising candidate for protein-polymer conjugation, due to the binding specificity and the reversibility upon pH change or the addition of imidazole or ethylenediaminetetraacetic acid (EDTA).^{18,19} Also, no modification of the protein is required as most recombinant therapeutic

proteins expressed by E.coli incorporate his tag (His₆) for affinity purification, which can also directly coordinate the NTA-Meⁿ⁺. Unfortunately, to the best of our knowledge, there is only one study published using NTA-Meⁿ⁺-His₆ for the formation of protein-polymer conjugates for protein therapy, but the conjugates were shown to exhibit low stability due to the poor binding

1
2
3 affinity.¹⁶ Supramolecular entities with two or three NTA heads (bisNTA and trisNTA,
4
5 respectively) exhibit improved binding affinity towards His-tagged proteins, and have been used
6
7 recently for the formation of protein-polymer conjugates.^{16,20} Among them, trisNTA possesses
8
9 the highest binding affinity,^{19,21-24} but the stability and the pH-triggered releaseability of trisNTA-
10
11 Me^{2+} -His₆ protein-polymer conjugates is still unknown.
12
13

14
15 Moreover, most protein-polymer conjugate systems allow for only one protein to be bound to
16
17 each or multiple polymers.^{7,25} Binding multiple proteins on each polymer would be able to
18
19 enhance the stability of conjugates due to the inter-protein interactions, similar to many natural
20
21 stabilized protein assemblies.²⁶⁻²⁸
22
23

24
25 A previous study published by our group introduced poly(N-isopropylacrylamide-*co*-tris-
26
27 nitrilotriacetic acid acrylamide) copolymers (PNTn, where n represents the mol% of trisNTA on
28
29 the polymer) containing Cu^{2+} for specific binding of His-tagged molecules.²⁰ Here, we employ
30
31 PNTn copolymers and His₆-eYFP (Figure 1) as models for polymer-protein conjugation to
32
33 analyze the effect on the stability, pH-triggered dissociation, and toxicity when variables such as
34
35 the nature of the metal, the distance between trisNTA sites, and the addition of inter-protein
36
37 interactions were varied. Three metal cations, Cu^{2+} , Zn^{2+} , and Fe^{3+} , were chosen as the
38
39 coordination center in the trisNTA pocket to modulate the binding affinity of His-tagged proteins
40
41 to the polymer, and were assessed by isothermal titration calorimetry (ITC). Then their ability to
42
43 reversibly bind based on changes in pH was analyzed by fast protein liquid chromatography
44
45 (FPLC). Also, the protein stability before and after conjugation, as well as after pH mediated
46
47 release, were measured by circular dichroism (CD) and fluorescence spectroscopy. Our strategy
48
49 of multiple protein conjugation to each polymer chain, and release upon pH changes can be
50
51
52
53
54
55
56
57
58
59
60

expanded to other systems, and advance the application of non-covalent interactions for protein-polymer conjugation.

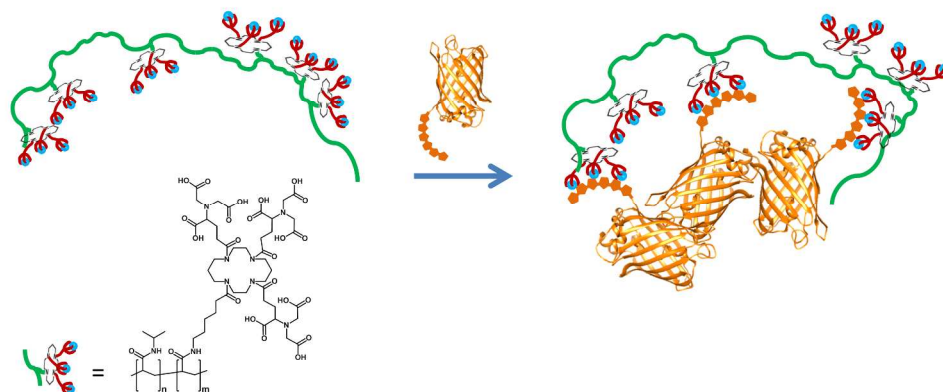


Figure 1. Schematic representation of site-specific conjugation of poly(N-isopropylacrylamide-*co*-tris-nitrilotriacetic acid acrylamide) polymers (green), which coordinate metals (blue) with His-tagged proteins (orange).

EXPERIMENTAL SECTION

Materials. Copper(II) chloride, zinc chloride, iron(III) sulfate hydrate, Dulbecco's modified eagle medium (DMEM) and phosphate buffered saline (PBS) were purchased from Sigma-Aldrich and used as received. 3-(4,5-dimethylthiazol-2-yl)-5-(3-carboxymethoxyphenyl)-2-(4-sulfophenyl)-2H-tetrazolium (MTS) was purchased from Promega, USA. Penicillin, streptomycin and fetal bovine serum (FBS) were purchased from Life technologies. Rhodamine B labelled hexahistidine (RHB-His₆) was received as a gift from Dr. Thomas Schuster. PierceTM BCA Protein Assay was from Thermo Scientific. All chemicals were purchased with the highest purity and used without further purification unless otherwise stated.

Chelation of metal cations to PNTn copolymers. Respective PNTn (0.2 mg/mL) were dissolved in PBS, pH 7.4. A stoichiometric excess of CuCl_2 , ZnCl_2 , or $\text{Fe}_2(\text{SO}_4)_3$ was mixed with the respective PNTn solution and was purified on a HiTrap desalting column (5 mL, GE Healthcare Life Sciences) with PBS as the mobile phase.

Protein expression and analysis. The expression of His₆-eYFP was performed as previously published.²⁹ The concentration of His₆-eYFP was determined by BCA protein assay and measured absorbance at 562 nm.

CD spectra were recorded using AVIV and Applied Photophysics Chirascan CD spectrophotometers at 25 °C with a time constant of 5 s and a step resolution of 1 nm in a 1mm quartz cell. CD data are given as mean of residual molar ellipticities ($\text{deg cm}^2 \text{ dmol}^{-1}$). The spectra are the result of 2-4 repeats. All measured solutions contained a final concentration of 4 μM His₆-eYFP protein in PBS, where the PBS background spectrum was subtracted.

Fluorescence of 100 nM His₆-eYFP ($\lambda_{\text{ex}} = 513 \text{ nm}$, $\lambda_{\text{em}} = 524 \text{ nm}$) and polymer-protein conjugates was investigated with a PerkinElmer LS55 fluorescence spectrometer (Waltham, Massachusetts, USA) at ambient temperature. Fluorescence of 60 nM RHB-His₆ alone ($\lambda_{\text{ex}} = 554 \text{ nm}$, $\lambda_{\text{em}} = 585 \text{ nm}$) and in complex with NTA-Cu^{2+} , trisNTA-Cu^{2+} and PNT4-Cu^{2+} was measured similarly.

Binding ability and affinity of His₆-eYFP to PNTn-Me²⁺ copolymers. Binding stoichiometry and dissociation constant (K_D) were determined by ITC. ITC was carried out using a VP-ITC microcalorimeter from MicroCal. Interaction constants characterizing the PNTn-Me²⁺ copolymers and His₆-eYFP were determined by direct titration of His₆-eYFP into polymer solutions in PBS pH 7.4 at 25°C. The concentration of His₆-eYFP and trisNTA on PNTn was 70 μM and 6 μM , respectively. During analysis the solution in the sample cell was stirred at 300

rpm. The volume of the sample cell and syringe were 1.4 mL and 295 μ L, respectively. Small aliquots of His₆-eYFP (typically 10 μ L) were added into the stirring solution over 240 s to allow complete equilibration. The first injection was set to a volume of 1 μ L to avoid air in the syringe and ignored for data analysis. Exothermic heat pulse (upper panel, Figure S1) that corresponds to an injection of 10 μ L of 70 μ M His₆-eYFP to 1.4 mL of 6 μ M trisNTA functional group on copolymers was recorded as a function of time. The data were analyzed using the Origin software package supplied by MicroCal and fitted by standard single-site binding model (lower panel, Figure S1). The stoichiometry value is equal to the value of the molar ratio for which the slope of the plot in lower panel is steepest. The slope of the plot at this point gives the value of the reciprocal of the dissociation constant.

Stability and pH-triggered dissociation of PNTn-Me²⁺-His₆-eYFP conjugates. FPLC was used for the analysis of the stability and the pH responsiveness of PNTn-Me²⁺-His₆-eYFP conjugates. 250 μ M His₆-eYFP was incubated with a metal cation-coordinated PNTn in PBS with a molar ratio of 1 : 2 for His₆-eYFP : trisNTA. The solution (500 μ L) was loaded onto a Superdex 200 10/300 GL (Akta Prime system, Amersham Biosciences, measuring @ 513 nm), and eluted with a PBS mobile phase. For the investigation of pH responsiveness, the column was equilibrated with PBS solution at pH 5.0 or 6.0. The sample was prepared in the same way as previously described, loaded onto the column and eluted with PBS solution at pH 5.0 or 6.0. The data were analyzed by Fityk software to calculate the integral area of the individual peaks.

Structure of PNTn-Me²⁺-His₆-eYFP conjugates. The size of PNTn-Me²⁺-His₆-eYFP conjugates were investigated by dynamic light scattering (DLS) with a Zetasizer Nano ZSP (Malvern Instruments Ltd., UK) at 25 °C in PBS. The data were fit based on number distribution. The concentration of His₆-eYFP was 20 μ M and 800 μ L of solution was used for measurements.

The negatively stained image of PNT4-Zn²⁺-His₆-eYFP conjugates (0.1 mg/mL, 5 μL) stained with 2% uranyl acetate was performed on a transmission electron microscope (Philips CM100) at an acceleration voltage of 80 kV. The size of the conjugates was analyzed using ImageJ software.

Cell culture. Hela cells or U87 glioblastoma cells were maintained at 37 °C in a 5% CO₂ humidified atmosphere and were grown in DMEM with 10% FBS, 100 units/mL penicillin, 100 μg/mL streptomycin and 2 mM L-glutamine.

Cell viability. Cytotoxicity testing was performed using the PromegaCellTiter 96 AQueous Non-Radioactive Cell Proliferation (MTS) assay (Promega, USA) to determine the number of viable cells in culture. Hela and U87 cells were seeded in a 96-well plate the night before experiments at 0.5×10^4 and 1×10^4 cells/well in 100 μl, respectively. The day of the experiment, samples (10μL) containing different amount of PNT4-Me²⁺ (0-375 μg/mL), were added to the cells. Twenty-four hours later, 20 μL of MTS solution were added to each well and incubated for 3h at 37 °C. Cell viability was calculated by measuring the absorbance at 490 nm using a 96-well plate reader and plotted relative to untreated cells that were grown the same day in the same plate and assays were performed in triplicate.

RESULTS AND DISCUSSION

Binding stoichiometry of His₆-eYFP to PNTn coordinated with different metal cations. PNT copolymers were previously synthesized and the average distance between trisNTA binding sites of PNT1, PNT2, PNT4, and PNT7 of 31.5 nm, 13.2 nm, 5.2 nm and 4.3 nm, were theoretically calculated, assuming an idealized linear polymer chain, by dividing the length of the polymer chain by the corresponding metal content. These calculations resulted in an average number of 2,

4, 7 and 9 trisNTA per polymer, respectively (Table S1).²⁰ Here we are interested to modulate the binding affinity of His-tagged proteins to these polymer chains decorated with tris-NTA groups, and in this respect, we selected three different metal cations, Cu^{2+} , Zn^{2+} , or Fe^{3+} . The binding stoichiometry of His₆-eYFP to the PNT-Meⁿ⁺ was assessed by ITC in order to calculate the dependence of the metal and of the distance between trisNTA sites on binding stoichiometry (Figure 2, S1). His₆-eYFP coordinated the Cu^{2+} or Zn^{2+} metals on PNTn copolymers with a maximum binding stoichiometry approaching 0.9:1 or 0.85:1, respectively, when the average distance between trisNTA binding sites was larger than the size of His₆-eYFP and steric hindrance did not block efficient binding. However, even though PNT7 has a higher content of trisNTA-Me²⁺ sites, a lower binding stoichiometry was observed (0.55 and 0.53 His₆-eYFP to trisNTA- Cu^{2+} and trisNTA- Zn^{2+} sites) due to steric hindrance, resulting from the coil conformation of the polymer in solution. In the case of PNTn containing trisNTA- Fe^{3+} , no coordination of His₆-eYFP was observed by ITC even when a high concentration of His₆-eYFP (180 μM) was added (data not shown).

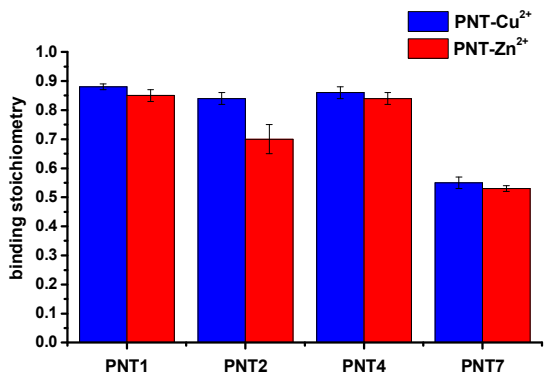


Figure 2. Binding stoichiometry between trisNTA-Me²⁺ in PNTn and His₆-eYFP.

Binding affinity of His₆-eYFP to PNTn-Me²⁺ copolymers. In addition to calculating the binding stoichiometry, the binding affinity of His₆-eYFP to PNTn containing either Cu²⁺ or Zn²⁺ was compared where the K_D value was normalized per NTA functional group per polymer chain to allow for comparison between the polymers containing different average number of binding sites. Similar to PNTn-Cu²⁺ (0.09-0.39 μ M), K_D values for PNTn-Zn²⁺-His₆-eYFP depended on the average distance between trisNTA binding sites. When the distance was decreased from 31.5 nm to 4.3 nm (PNT1-Zn²⁺-His₆-eYFP and PNT7-Zn²⁺-His₆-eYFP, respectively), the K_D values decreased from 1.35 ± 0.12 μ M to 0.46 ± 0.06 μ M. It is known that numerous factors play a role in the binding strength of a metal to its coordination pocket including size, charge, protein oligomerization and other stabilizing or destabilizing interactions.³⁰⁻³³ For example, increasing the number of binding sites could decrease the K_D of a small molecule due to a decreased rate of dissociation. On the contrary if the size of proteins is larger than the mean distance between trisNTA-Meⁿ⁺ sites, the binding affinity is decreased even if an increased number of coordination is present due to steric hindrance and charge repulsion of the protein.²⁰ However, increasing the number of trisNTA-Me²⁺ per polymer, effectively decreasing their separation, stabilized the conjugate. While many factors play a role in affinity, this decrease of K_D supports the previous findings that a decrease of enthalpy was seen upon binding of PNT4 compared to PNT1 copolymers indicating an increase in hydrogen bond formation from inter-protein interactions.³⁰⁻³³ This led to a binding affinity dependency of PNTn-Me²⁺-His₆-eYFP based on a combined effect between the coordination strength of the metal and the amount of inter-protein interactions, which overcomes the coil-hindrance (Figure 3).

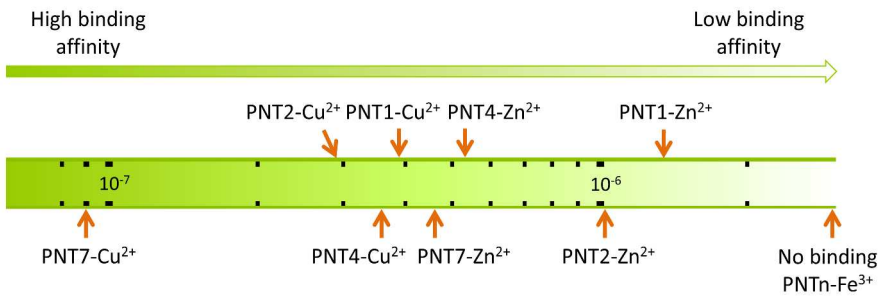


Figure 3. K_D (M) for the binding between PNTn- Cu^{2+} / Zn^{2+} / Fe^{3+} and His₆-eYFP at pH = 7.4.

The binding affinity of His-tagged proteins is dependent on the strength of coordination with the metal where $\text{Cu}^{2+} > \text{Ni}^{2+} > \text{Zn}^{2+} > \text{Fe}^{3+}$.³⁴ Therefore, Zn^{2+} is rarely used for NTA conventional applications, such as purification of proteins, due to its poor binding affinity ($\log_{10}K = 3.25 \text{ M}^{-1}$).³⁵ Even with the increased binding created by using trisNTA instead of NTA or bisNTA, it is apparent that when inter-protein interactions are not present, as is the case for PNT1, the binding affinity with Zn^{2+} is still much weaker than its Cu^{2+} equivalent. By increasing the inter-protein interactions as a result of an increased number of accessible trisNTA coordination pockets, the binding affinity increases due to stabilization of the conjugates. However, for PNT7 the steric hindrance leads to a decrease in binding stoichiometry as described above. Introducing inter-protein interactions leads to more stable Zn^{2+} conjugates, which makes them suitable for further applications (Figure 3). This strategy is seen in nature to stabilize self-assembled structures by inter-protein interactions.²⁶⁻²⁸

Physical characteristics of PNTn- Me^{2+} -His₆-eYFP conjugates and protein stability. The size of PNTn- Me^{2+} -His₆-eYFP conjugates was characterized by DLS. PNT1- Cu^{2+} / Zn^{2+} and PNT4- Cu^{2+} / Zn^{2+} were chosen as representative polymers for further investigations including size measurements and stabilities in various pHs. Even though PNT1 has an average number of 2 trisNTA- Me^{2+} binding sites per polymer, in order to compare a multiple protein system to the

classical one protein per PNT1, a 2 : 1 ratio of trisNTA-Me²⁺ to His₆-eYFP was chosen. Also, since the binding studies showed a stoichiometry < 1 for PNTn polymers to the average number of binding sites, this means each polymer solution has a mixture of polymers containing an average number of accessible binding sites less than the theoretical value (2 for PNT1, and 7 for PNT4). Therefore, this 2 : 1 ratio was used for both PNTn to keep the number of proteins proportional on each polymer chain. For this molar ratio, there are an average of 3 or 4 His₆-eYFPs per polymer chain for PNT4, and an average of one His₆-eYFP per polymer chain for PNT1. In addition, due to the excess of trisNTA-Me²⁺ compared to His₆-eYFP, no free proteins are expected.

In order to directly measure the size shift of the tertiary structure of polymer chains in solution due to the binding of proteins, dynamic light scattering was performed. The hydrodynamic diameter (D_H) of His₆-eYFP was determined to be 5.0 ± 0.9 nm. The D_H of PNT1-Zn²⁺ was 8.1 ± 2.5 nm and when coordinated with His₆-YFP increased in size to 9.7 ± 2.4 nm (Figure S3). PNT4-Zn²⁺ was 5.8 ± 1.8 nm (Figure S2) and after binding, the diameter value shifted to 13.1 ± 2.8 nm, which was similar to PNT4-Cu²⁺-His₆-eYFP (data not shown). The change in size between PNT1-Zn²⁺ and PNT4-Zn²⁺ after binding His₆-eYFP can be explained by the increased average number of proteins per polymer. The DLS data was supported with transmission electron microscopy (TEM), revealing structures with a diameter of 12 ± 3 nm for PNT4-Zn²⁺-His₆-eYFP (Figure S4).

To address the question of whether the conjugation of polymers to proteins causes alterations in their secondary structure, His₆-eYFP was characterized before and after polymer conjugation by CD spectroscopy. The far-UV CD spectra of His₆-eYFP and PNT1/4-Zn²⁺-His₆-eYFP, showed

that conjugation did not alter the protein structure (Figure S5), agreeing with the previously published results.^{20,36}

PNTn-Me²⁺-His₆-eYFP stability under varying pHs. The stability of PNTn-Me²⁺-His₆-eYFP conjugates under various pH's was investigated by FPLC. Each of the protein-polymer conjugates were measured to establish a baseline of the amount of free His₆-eYFP in each and calculated as a percent of intact protein-polymer complex (Figure 4,). PNT1-Cu²⁺-His₆-eYFP showed a lower stability than PNT4-Cu²⁺-His₆-eYFP at pH 7.4 (Figure S6). The difference between PNT1-Zn²⁺-His₆-eYFP and PNT4-Zn²⁺-His₆-eYFP was even more significant with only 46.6% of His₆-eYFP remaining bound with PNT1-Zn²⁺ while 80.2% of His₆-eYFP remaining complexed with PNT4-Zn²⁺. Because PNTn-Me²⁺ copolymers are highly negatively-charged,²⁰ the potential electrostatic interactions between protein-polymer conjugates and gel filtration media might decrease the stability of conjugates during the FPLC analysis.³⁷⁻³⁹ This was tested by increasing the number of available PNT4-Zn²⁺ from 2 to 10 equivalents compared to His₆-eYFP. Even with a 5 fold increase in potential interaction sites, the % of free protein remained the same suggesting that the phenomena was caused by interaction with the column (Figure S7). The higher stability of PNT4-Me²⁺-His₆-eYFP compared to PNT1-Me²⁺-His₆-eYFP is attributed to inter-protein interactions preventing the disassociation of the complex, in agreement with the binding affinity values. Inter-protein interactions stabilize the protein-polymer conjugates when the number of trisNTA groups is increased (PNT4 compared with PNT1) strengthening the interaction when the metal is not a strong coordination center (Zn²⁺).

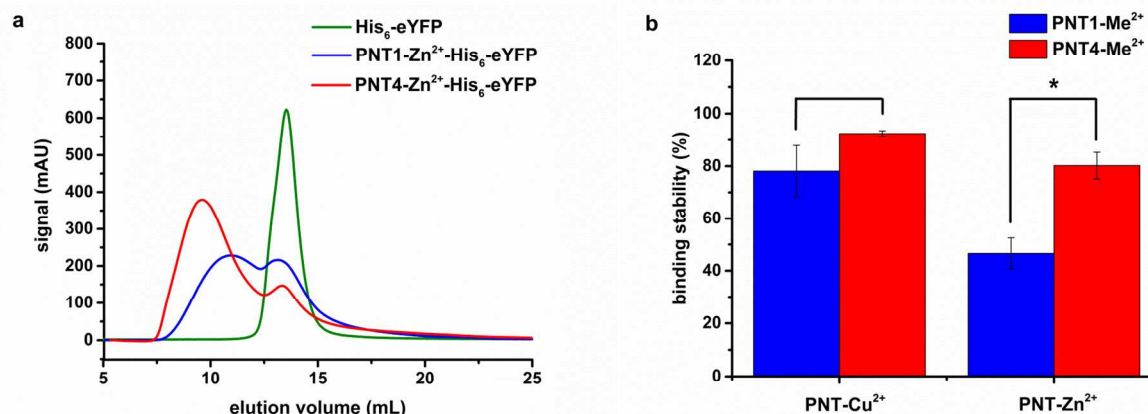


Figure 4. Stability of PNTn-Me²⁺-His₆-eYFP conjugates at pH 7.4. (a) FPLC chromatograms of His₆-eYFP and PNT1/4-Zn²⁺-His₆-eYFP. (b) The percentage of His₆-eYFP bound with PNT1/4-Me²⁺. Stars indicate significance in two-tailed Student's t-test; *P<0.05, n=3.

An attractive property of NTA-Me²⁺-His₆ molecular recognition is pH sensitive binding.¹⁸ However, this property has previously not been proven with trisNTA protein-polymer conjugates. In order to investigate the pH sensitive binding, a model peptide, hexahistidine labeled with Rhodamine B (RHB-His₆) was used to compare the parameters that effect binding stability across various pHs. RHB-His₆ is strongly quenched when bound to Cu²⁺, and more stable than eYFP at lower pH.⁴⁰ The binding of trisNTA-Cu²⁺ to RHB-His₆ resulted in a significant decrease of fluorescent intensity from 570 to 60. The fluorescent intensity remained unchanged at all pH > 3.5 (Figure S8), indicating that the binding between trisNTA-Cu²⁺ and RHB-His₆ is stable at various pHs. PNT4-Cu²⁺-RHB-His₆ exhibited no dissociation with pH > 3.5, suggesting that the presence of polymer does not significantly influence the binding stability. Also, PNT4-Cu²⁺ did not show a significant release of His₆-eYFP when the pH was changed from 7.4 to 6.0, but 52% of the conjugates disassociated at pH 5.0, respectively (Figure 5). As expected, due to the lack of inter-protein interactions, the release of His₆-eYFP was more

pronounced for PNT1-Cu²⁺ at pH values down to 6, ending at pH =5 to a similar fraction of dissociated conjugates (53%). The higher percent of pH-triggered dissociation can be attributed the higher K_D at pH 7.4 of PNT4-Cu²⁺-His₆-eYFP ($K_D=0.36\ \mu\text{M}$) compared with PNT4-Cu²⁺-RHB-His₆ ($K_D=0.13\ \mu\text{M}$).²⁰ In contrast with PNTn-Cu²⁺, both PNT1-Zn²⁺ and PNT4-Zn²⁺ exhibited a more rapid dissociation. At pH 7.4 PNT1-Zn²⁺ and PNT4-Zn²⁺ dissociated from His₆-eYFP at 53.4% compared to 19.8% determined by FPLC, respectively. Decreasing the pH to 6.0 increased the dissociation of His₆-eYFP from PNT1-Zn²⁺ and PNT4-Zn²⁺ to 92% and 76%, respectively, with both conjugates being completely unbound by pH 5.0 (Figure 5 a, b). The higher dissociation of PNTn-Zn²⁺-His₆-eYFP compared with PNTn-Cu²⁺-His₆-eYFP at lower pH was expected, due to the higher K_D values (0.46-1.35 μM , 0.09-0.39 μM , respectively). The trisNTA-Cu²⁺ binding sites on PNTn have stronger interaction with His₆-eYFP compared with protons ($K_D \approx 1\ \mu\text{M}$),^{18,41} therefore it is difficult to be protonated to induce the dissociation of the proteins. However, the affinity of trisNTA-Zn²⁺ on PNTn to His₆-eYFP is comparable to that of protons, resulting in direct competition between protonation and coordination of the His₆-eYFP. This led to PNTn-Zn²⁺-His₆-eYFP having a higher amount of pH-triggered release than PNT-Cu²⁺-His₆-eYFP. Furthermore, the reversibility of pH dependent binding of PNT4-Zn²⁺-His₆-eYFP was investigated due to its higher pH binding dependence. A solution of PNT4-Zn²⁺-His₆-eYFP was formed in pH 7.4 and tested for stability, the pH was then decreased to 5.0 and dissociation was observed. However, when the pH was increased back to pH 7.4 almost complete reformation of all protein complexes was observed (Figure 5c).

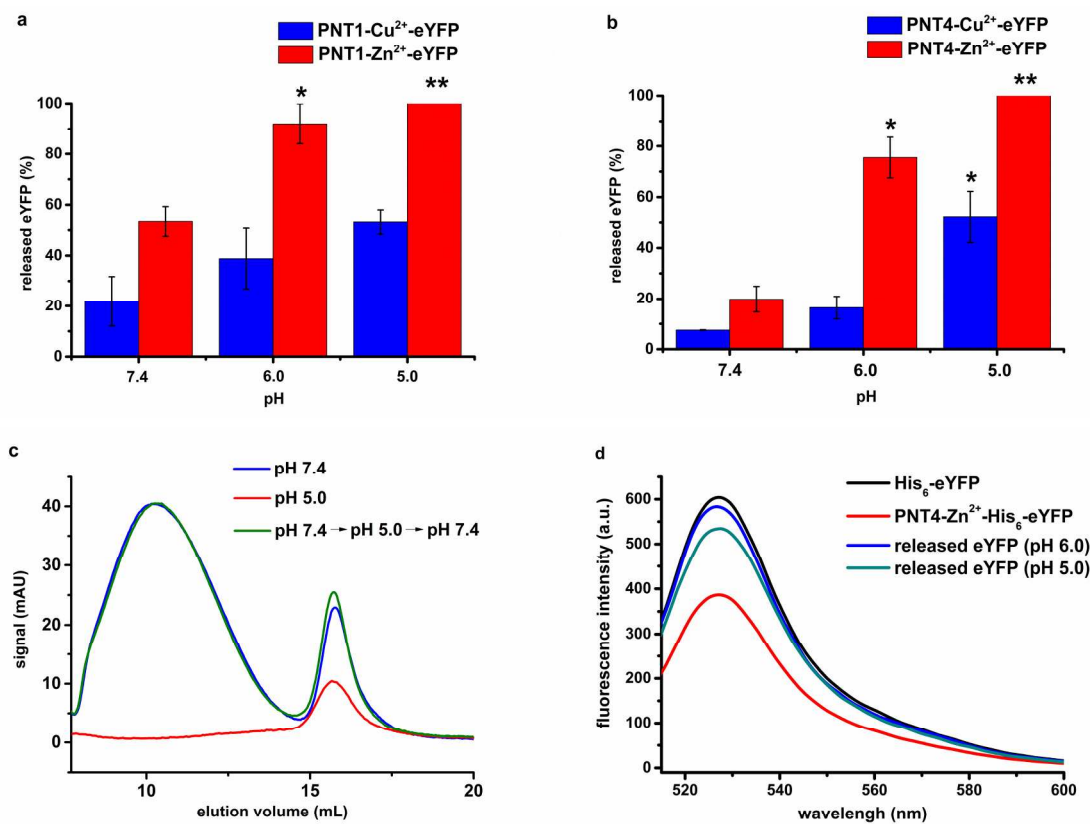


Figure 5. Release of His₆-eYFP from PNT1-Me²⁺ (a) and PNT4-Me²⁺ (b) at different pH values. All statistics were analyzed by comparing samples to their respective protein-polymer conjugate at pH 7.4. Stars indicate significance compared to the equivalent protein polymer conjugate at pH 7.4 in a two-tailed Student's t-test; *P<0.05, **P<0.005. (c) Reversibility of pH dependent binding between PNT4-Zn²⁺ and His₆-eYFP analyzed by FPLC. (d) The fluorescence emission spectra of His₆-eYFP and PNT4-Zn²⁺-His₆-eYFP before and after release in acidic conditions. While reactions were run in acidic conditions, all samples were analyzed at pH 7.4 in PBS.

To address the question of whether the reversible binding of PNTn copolymers to His₆-eYFP influence its fluorescent property, His₆-eYFP was characterized by fluorescence spectroscopy before and after polymer conjugation (Figure 5d). When His₆-eYFP was conjugated with PNT4-

Zn^{2+} , a decrease in fluorescence intensity was observed due to the chelation with Zn^{2+} . After dissociation from PNT4- Zn^{2+} in acidic conditions (pH = 5.0 or 6.0), the released His₆-eYFP was collected and then buffered back to pH 7.4, the fluorescence of His₆-eYFP recovered almost to its original value. The slight decrease of fluorescence intensity was due to short-term exposure to acidic condition which corresponds to literature precedence.⁴² In addition, the second structure of dissociated His₆-eYFP after buffering back pH 7.4 was evaluated by CD spectroscopy. No obvious change of the spectrum was observed, suggesting His₆-eYFP was kept intact during the pH-triggered dissociation (Figure S9). Therefore, PNTn copolymers are able to bind His₆-eYFP at physiological pH and release the bound protein in acidic conditions without influencing the structure and properties.

Cytotoxicity evaluation of PNT4-Meⁿ⁺ copolymers. The cytotoxicity of PNT4-Meⁿ⁺ copolymers was evaluated on U87 and HeLa cells by using the MTS assay (Figure 6). PNT4 copolymer showed low toxicity in all range of concentrations tested in both cell lines. The coordination of PNT4 with Zn^{2+} did not induce toxicity in contrast to PNT4 coordinated with Cu^{2+} or Ni^{2+} that showed toxicity with increasing concentrations (Figure S10). trisNTA coordinated with Cu^{2+} , Ni^{2+} , Zn^{2+} was tested as a control and showed slightly higher toxicity compared to equivalent copolymer samples (Figure S10). Repeat administrations of Cu^{2+} or Ni^{2+} can accumulate in the liver, kidney, and spleen, leading to organ damage after the complex has dissociated and the metal released.⁴³⁻⁴⁶ Therefore in terms of its low toxicity, a protein-polymer conjugate comprised of PNT4 and Zn^{2+} would be suitable for further in vitro studies.

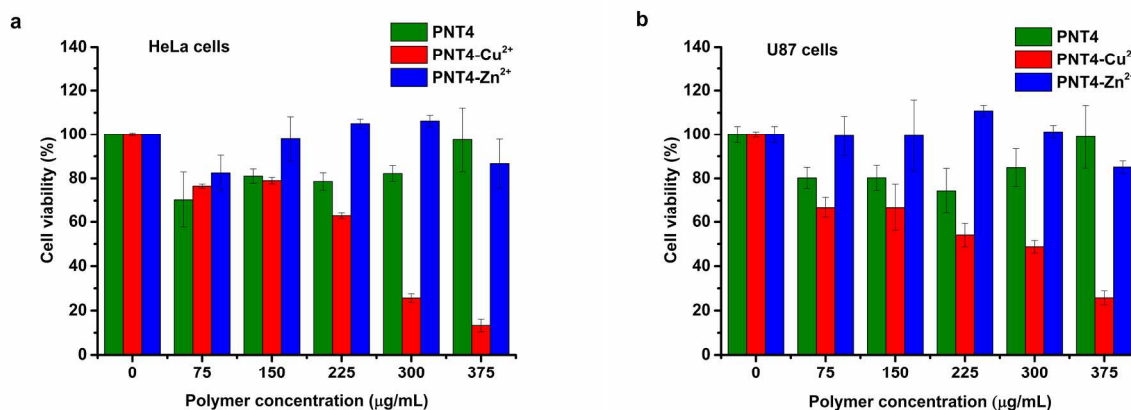


Figure 6. Toxicity evaluation of PNT4-Meⁿ⁺ copolymers on HeLa (a) and U87 (b) cells using MTS assay where zero polymer concentration refers to the addition of PBS to the cells. Errors bars represent the standard deviation (n=3).

CONCLUSION

An efficient method to site-specifically and reversibly bind multiple proteins per polymer chain using trisNTA-Me²⁺-His₆ molecular recognition was designed. His₆-eYFP was used as a model protein for binding PNT-Meⁿ⁺ copolymers. It was demonstrated that the nature of the Meⁿ⁺ and the number of metal binding pockets of trisNTA enable great selectivity for the binding affinity. This led to control of the stability and pH triggered release of the protein from the polymer by modulating inter-protein interactions. After complete release of His₆-eYFP from PNT-Me²⁺ copolymers at selective pH, the return of fluorescence suggested that the protein was intact and maintained its properties. In addition, the toxicity problem of trisNTA-Meⁿ⁺ and its derivatives, has been improved by using Zn²⁺, which still maintained the binding with His₆-eYFP due to controllable inter-protein interactions.

The presented system advances the field from covalent single protein-polymer conjugates to non-covalent multiple protein-polymer conjugates that can be readily formed and dissociated

dependent on pH, and serves as a platform for the combination of various active agents into one nanosystem to potentially fulfill multiple tasks such as therapy and diagnosis in a combined manner.

ASSOCIATED CONTENT

Supporting information

Characterization of protein-polymer conjugates, additional cell toxicity data, fluorescent spectra of trisNTA-Cu²⁺-RHB-His₆ in various pH and CD spectra of His₆-eYFP. This material is available free of charge via the Internet at <http://pubs.acs.org>.

AUTHOR INFORMATION

Corresponding Authors

* tel: +41 (0)61 267 38 39; fax: +41 (0)61 267 38 55; cornelia.palivan@unibas.ch

* tel: +41 (0)61 267 38 02; fax: +41 (0)61 267 38 55; wolfgang.meier@unibas.ch

Notes

The authors declare no competing financial interest.

ACKNOWLEDGMENT

We thank Swiss National Science Foundation and University of Basel for financial support. J. L. thanks China Scholarship Council for supporting the fee to study abroad. We thank Biozentrum Biophysics Facility Basel for the use of their ITC instrument. J. L. thanks Mariana Spulber from University of Basel for extensive discussions.

REFERENCES

- (1) Leader, B.; Baca, Q. J.; Golan, D. E. Protein Therapeutics: a Summary and Pharmacological Classification. *Nat. Rev. Drug Discov.* **2008**, *7*, 21-39.
- (2) Frokjaer, S.; Otzen, D. E. Protein Drug Stability: a Formulation Challenge. *Nat. Rev. Drug Discov.* **2005**, *4*, 298-306.
- (3) De Groot, A. S.; Scott, D. W. Immunogenicity of Protein Therapeutics. *Trends Immunol.* **2007**, *28*, 482-490.
- (4) Duncan, R. Polymer Conjugates as Anticancer Nanomedicines. *Nat. Rev. Cancer.* **2006**, *6*, 688-701.
- (5) Knop, K.; Hoogenboom, R.; Fischer, D.; Schubert, U. S. Poly(ethylene glycol) in Drug Delivery: Pros and Cons as Well as Potential Alternatives. *Angew. Chem., Int. Ed.* **2010**, *49*, 6288-6308.
- (6) Kolate, A.; Baradia, D.; Patil, S.; Vhora, I.; Kore, G.; Misra, A. PEG - a Versatile Conjugating Ligand for Drugs and Drug Delivery Systems. *J. Control. Release* **2014**, *192*, 67-81.
- (7) Pelegri-O'Day, E. M.; Lin, E.-W.; Maynard, H. D. Therapeutic Protein-Polymer Conjugates: Advancing Beyond PEGylation. *J. Am. Chem. Soc.* **2014**, *136*, 14323-14332.
- (8) Harris, J. M.; Chess, R. B. Effect of Pegylation on Pharmaceuticals. *Nat. Rev. Drug Discov.* **2003**, *2*, 214-221.
- (9) Gauthier, M. A.; Klok, H.-A. Polymer-Protein Conjugates: an Enzymatic Activity Perspective. *Polym. Chem.* **2010**, *1*, 1352-1373.

- (10) Secundo, F. Conformational Changes of Enzymes upon Immobilisation. *Chem. Soc. Rev.* **2013**, *42*, 6250-6261.
- (11) Filpula, D.; Zhao, H. Releasable PEGylation of Proteins with Customized Linkers. *Adv. Drug Deliv. Rev.* **2008**, *60*, 29-49.
- (12) Tao, L.; Liu, J.; Xu, J.; Davis, T. P. Bio-Reversible polyPEGylation. *Chem. Commun.* **2009**, 6560-6562.
- (13) Gong, Y.; Leroux, J.-C.; Gauthier, M. A. Releasable Conjugation of Polymers to Proteins. *Bioconjugate Chem.* **2015**, DOI: 10.1021/bc500611k.
- (14) Kulkarni, S.; Schilli, C.; Grin, B.; Müller, A. H. E.; Hoffman, A. S.; Stayton, P. S. Controlling the Aggregation of Conjugates of Streptavidin with Smart Block Copolymers Prepared via the RAFT Copolymerization Technique. *Biomacromolecules* **2006**, *7*, 2736–2741.
- (15) Chen, J.; Zhao, M.; Feng, F.; Sizovs, A.; Wang, J. Tunable Thioesters as “Reduction” Responsive Functionality for Traceless Reversible Protein PEGylation. *J. Am. Chem. Soc.* **2013**, *135*, 10938-10941.
- (16) Kim, T. H.; Swierczewska, M.; Oh, Y.; Kim, A.; Jo, D. G.; Park, J. H.; Byun, Y.; Sadegh-Nasseri, S.; Pomper, M. G.; Lee, K. C. **et al.** Mix to Validate: a Facile, Reversible PEGylation for Fast Screening of Potential Therapeutic Proteins In Vivo. *Angew. Chem., Int. Ed.* **2013**, *52*, 6880-6884.
- (17) Nguyen, T. H.; Kim, S.-H.; Decker, C. G.; Wong, D. Y.; Loo, J. A.; Maynard, H. D. A Heparin-Mimicking Polymer Conjugate Stabilizes Basic Fibroblast Growth Factor. *Nat Chem.* **2013**, *5*, 221-227.

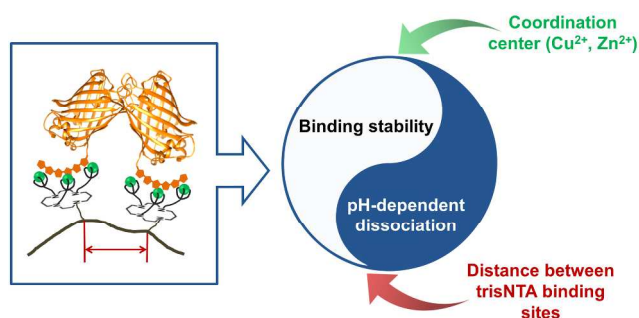
- (18) June, R. K.; Gogoi, K.; Eguchi, A.; Cui, X.-S.; Dowdy, S. F. Synthesis of a pH-Sensitive Nitrilotriacetic Linker to Peptide Transduction Domains to Enable Intracellular Delivery of Histidine Imidazole Ring-Containing Macromolecules. *J. Am. Chem. Soc.* **2010**, *132*, 10680-10682.
- (19) André, T.; Reichel, A.; Wiesmüller, K.-H.; Tampé, R.; Piehler, J.; Brock, R. Selectivity of Competitive Multivalent Interactions at Interfaces. *ChemBioChem* **2009**, *10*, 1878-1887.
- (20) Liu, J.; Spulber, M.; Wu, D.; Talom, R. M.; Palivan, C. G.; Meier, W. Poly(N-Isopropylacrylamide-co-Tris-Nitrilotriacetic Acid Acrylamide) for a Combined Study of Molecular Recognition and Spatial Constraints in Protein Binding and Interactions. *J. Am. Chem. Soc.* **2014**, *136*, 12607-12614.
- (21) Lata, S.; Reichel, A.; Brock, R.; Tampé, R.; Piehler, J. High-Affinity Adaptors for Switchable Recognition of Histidine-Tagged Proteins. *J. Am. Chem. Soc.* **2005**, *127*, 10205-10215.
- (22) Grunwald, C.; Schulze, K.; Reichel, A.; Weiss, V.; Blaas, D.; Piehler, J.; Wiesmüller, K.; Tampé, R. In Situ Assembly of Macromolecular Complexes Triggered by Light. *Proc. Natl. Acad. Sci. U.S.A.* **2010**, *107*, 6146.
- (23) Huang, Z.; Hwang, P.; Watson, D. S.; Cao, L.; Szoka, F. C. Tris-Nitrilotriacetic Acids of Subnanomolar Affinity Toward Hexahistidine Tagged Molecules. *Bioconjugate Chem.* **2009**, *20*, 1667-1672.

- (24) Nehring, R.; Palivan, C. G.; Casse, O.; Tanner, P.; Tu xen, J.; Meier, W. Amphiphilic Diblock Copolymers for Molecular Recognition: Metal-Nitrilotriacetic Acid Functionalized Vesicles. *Langmuir* **2008**, *25*, 1122-1130.
- (25) Broyer, R. M.; Grover, G. N.; Maynard, H. D. Emerging Synthetic Approaches for Protein-Polymer Conjugations. *Chem. Commun.* **2011**, *47*, 2212-2226.
- (26) Bolanos-Garcia, V. M.; Wu, Q.; Ochi, T.; Chirgadze, D. Y.; Sibanda, B. L.; Blundell, T. L. Spatial and Temporal Organization of Multi-Protein Assemblies: Achieving Sensitive Control in Information-Rich Cell-Regulatory Systems. *Phil. Trans. R. Soc. A* **2012**, *370*, 3023-3039.
- (27) Nussinov, R.; Jang, H. Dynamic Multiprotein Assemblies Shape the Spatial Structure of Cell Signaling. *Prog. Biophys. Mol. Biol.* **2014**, *116*, 158-164.
- (28) Saka, S. K.; Honigsmann, A.; Eggeling, C.; Hell, S. W.; Lang, T.; Rizzoli, S. O. Multi-Protein Assemblies Underlie the Mesoscale Organization of the Plasma Membrane. *Nat. Commun.* **2014**, *5*, 4059.
- (29) Bruns N.; Pustelny K.; Bergeron L.; Whiehead T.; Ckark D. Mechanical Nanosensor Based on FRET Within a Thermosome: Damage-Reporting Polymeric Materials. *Angew. Chem., Int. Ed.* **2009**, *48*, 5666-5669.
- (30) Griffith, B. R.; Allen, B. L.; Rapraeger, A. C.; Kiessling, L. L. A Polymer Scaffold for Protein Oligomerization. *J. Am. Chem. Soc.* **2004**, *126*, 1608-1609.
- (31) Saluja, A.; Kalonia, D. S. Nature and Consequences of Protein-Protein Interactions in High Protein Concentration Solutions. *Int. J. Pharm.* **2008**, *358*, 1-15.
- (32) Van Rijn, P. Polymer Directed Protein Assemblies. *Polymers* **2013**, *5*, 576-599.

- (33) Cairo, W. C.; Gestwicki, E. J.; Kanai, M.; Kiessling, L. L. Control of Multivalent Interactions by Binding Epitope Density. *J. Am. Chem. Soc.* **2002**, *124*, 1615-1619.
- (34) Choe, W.-S.; Clemmitt, R. H.; Chase, H. A.; Middelberg, A. P. J. Comparison of Histidine-Tag Capture Chemistries for Purification Following Chemical Extraction. *J. Chromatogr. A* **2002**, *953*, 111-121.
- (35) Stadlbauer, S. Coordination Chemistry in Molecular Recognition. Ph.D. Dissertation, University of Regensburg, Regensburg, **2009**.
- (36) Xia, Y.; Tanga, S.; Olsen, B. D. Site-Specific Conjugation of RAFT Polymers to Proteins via Expressed Protein Ligation. *Chem. Commun.* **2013**, *49*, 2566-2568.
- (37) Pujar N. S.; Zydney A. L. Electrostatic Effects on Protein Partitioning in Size-Exclusion Chromatography and Membrane Ultrafiltration. *J. Chromatogr. A* **1998**, *796*, 229-238.
- (38) Arakawa T.; Ejima D.; Li T. S.; Philo J. S. The Critical Role of Mobile Phase Composition in Size Exclusion Chromatography of Protein Pharmaceuticlas. *J. Pharm. Sci.* **2009**, *99*, 1674-1692.
- (39) Stulik K.; Pacaova V.; Ticha M. Some Potentialities and Drawbacks of Contemporary Size-Exclusion Chromatography. *J. Biochem. Bioph. Methods* **2003**, *56*, 1-13.
- (40) Lata, S.; Gavutis, M.; Tampé, R.; Piehler, J. Specific and Stable Fluorescence Labeling of Histidine-Tagged Proteins for Dissecting Multi-Protein Complex Formation. *J. Am. Chem. Soc.* **2006**, *128*, 2365-2372.

- (41) Liu, T.; Ryan, M.; Dahlquist, F. W.; Griffith, O. H. Determination of pKa Values of the Histidine Side Chains of Phosphatidylinositol-Specific Phospholipase C from *Bacillus Cereus* by NMR Spectroscopy and Site-Directed Mutagenesis. *Protein Sci.* **1997**, *6*, 1937-1944.
- (42) Anderson, D. E.; Becktel, W. J.; Dahlquist, F. W. pH-Induced Denaturation of Proteins: a Single Salt Bridge Contributes 3-5 kcal/mol to the Free Energy of Folding of T4 Lysozyme. *Biochemistry* **1990**, *29*, 2403-2408.
- (43) Turnlund, J. R. Human Whole-Body Copper Metabolism. *Am. J. Clin. Nutr.* **1998**, *67*, 960S-964S.
- (44) Pereira, M. C.; Pereira, M. L.; Sousa, J. P. Evaluation of Nickel Toxicity on Liver, Spleen, and Kidney of Mice after Administration of High-Dose Metal Ion. *J. Biomed. Mater. Res.* **1998**, *40*, 40-47.
- (45) Gupta, S. Cell Therapy to Remove Excess Copper in Wilson's Disease. *Ann. N. Y. Acad. Sci.* **2014**, *1315*, 70-80.
- (46) Guo, H.; Wu, B.; Cui, H.; Peng, X.; Fang, J.; Zuo, Z.; Deng, J.; Wang, X.; Deng, J.; Yin, S. **et al.** NiCl₂-Down-Regulated Antioxidant Enzyme mRNA Expression Causes Oxidative Damage in the Broiler's Kidney. *Biol. Trace Elem. Res.* **2014**, *162*, 288-295.

Table of Contents Graphic



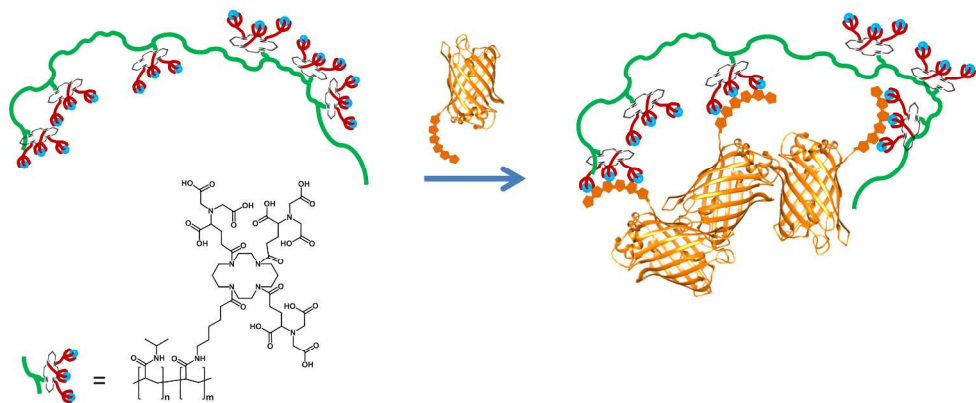


Figure 1. Schematic representation of site-specific conjugation of poly(N-isopropylacrylamide-co-tris-nitrilotriacetic acid acrylamide) polymers (green), which coordinate metals (blue) with His-tagged proteins (orange).
251x114mm (300 x 300 DPI)

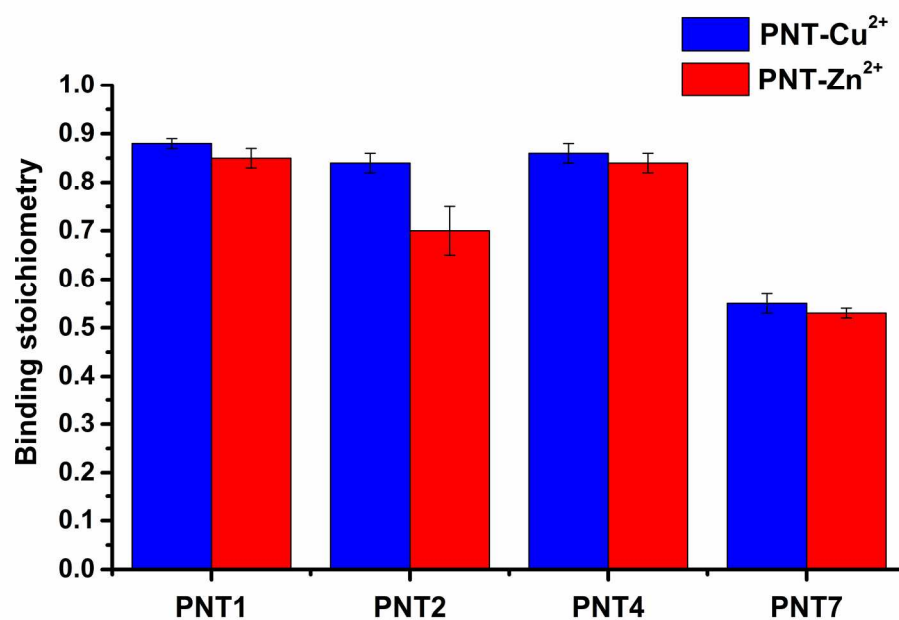


Figure 2. Binding stoichiometry between trisNTA- Me_2^+ in PNTn and His6-eYFP.
201x140mm (300 x 300 DPI)

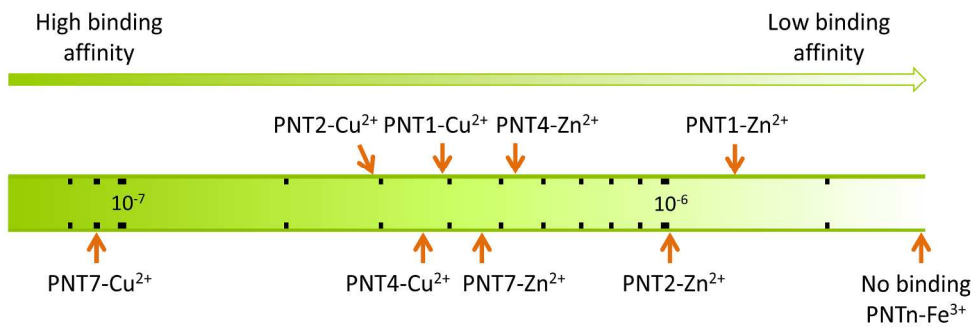


Figure 3. KD (M) for the binding between PNTn-Cu²⁺/Zn²⁺/Fe³⁺ and His6-eYFP at pH = 7.4.
253x87mm (300 x 300 DPI)

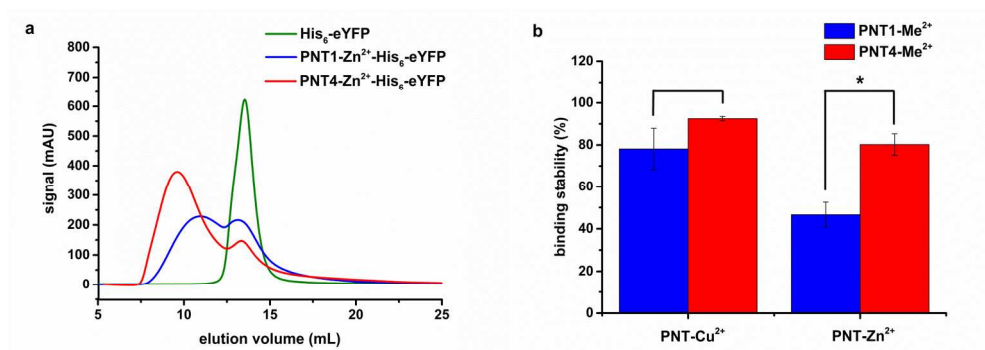


Figure 4. Stability of PNTn-Me²⁺-His₆-eYFP conjugates at pH 7.4. (a) FPLC chromatograms of His₆-eYFP and PNT1/4-Zn²⁺-His₆-eYFP. (b) The percentage of His₆-eYFP bound with PNT1/4-Me²⁺. Stars indicate significance in two-tailed Student's t-test; *P<0.05, n=3.

238x92mm (300 x 300 DPI)

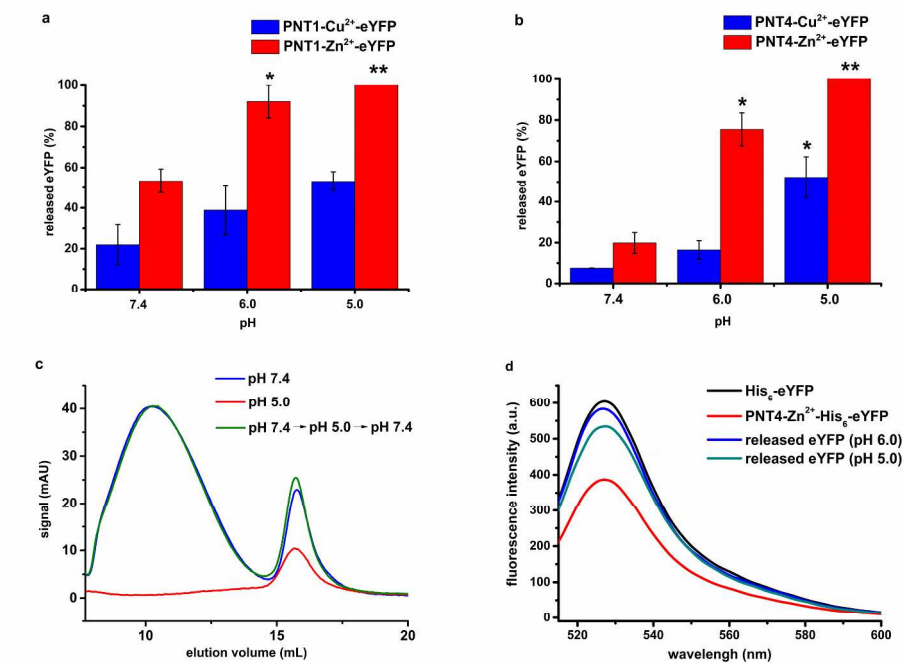


Figure 5. Release of His6-eYFP from PNT1-Me2+ (a) and PNT4-Me2+ (b) at different pH values. All statistics were analyzed by comparing samples to their respective protein-polymer conjugate at pH 7.4. Stars indicate significance compared to the equivalent protein polymer conjugate at pH 7.4 in a two-tailed Student's t-test; *P<0.05, **P<0.005. (c) Reversibility of pH dependent binding between PNT4-Zn2+ and His6-eYFP analyzed by FPLC. (d) The fluorescence emission spectra of His6-eYFP and PNT4-Zn2+-His6-eYFP before and after release in acidic conditions. While reactions were run in acidic conditions, all samples were analyzed at pH 7.4 in PBS.

254x190mm (300 x 300 DPI)

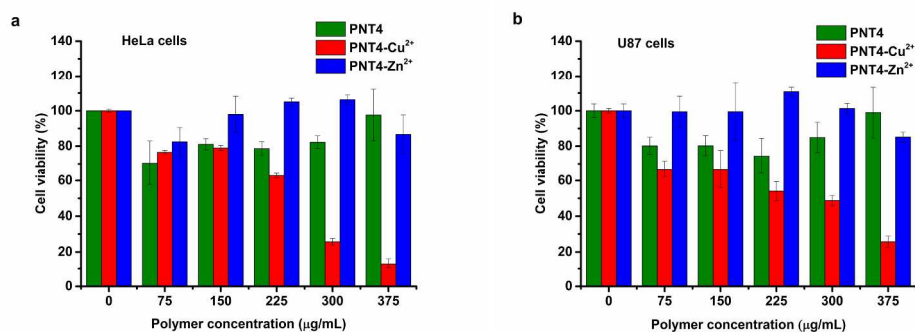
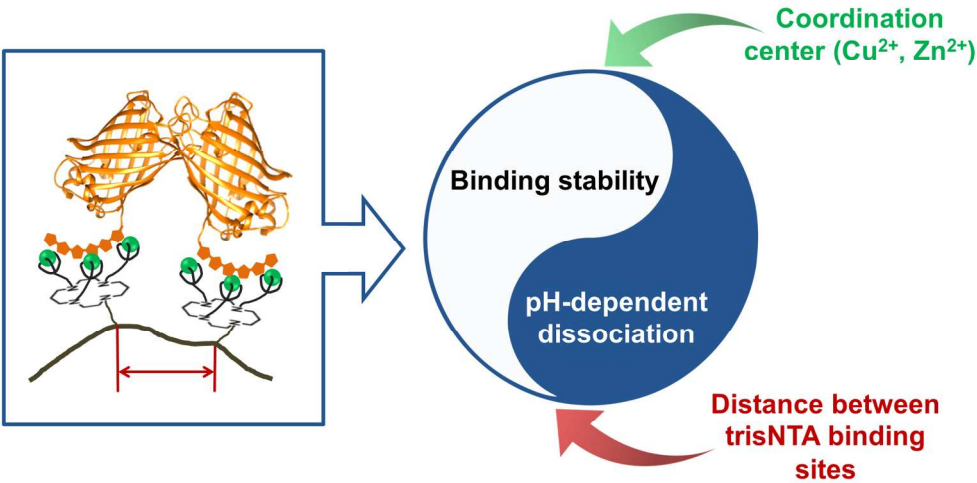


Figure 6. Toxicity evaluation of PNT4-Men⁺ copolymers on HeLa (a) and U87 (b) cells using MTS assay where zero polymer concentration refers to the addition of PBS to the cells. Errors bars represent the standard deviation (n=3).
244x91mm (300 x 300 DPI)



Graphical abstract
325x175mm (150 x 150 DPI)